Journal of Alloys and Compounds, 189 (1992) 145–149
JALNEW 337

The misch metal–iron system

M. Uma Devi and K. P. Gupta
Department of Metallurgical Engineering, Indian Institute of Technology, Kanpur 208016 (India)

(Received October 11, 1991; in final form March 30, 1992)

Abstract

The misch metal–iron (MM–Fe) system has been investigated in the temperature range from 700 to 1150 °C at the iron-rich end (up to 33.3% RE, where RE is the total rare earth content of the MM). Two intermediate phases, $Fe_{17}RE_2$ and Fe_2RE, and two broad three-phase fields, α-Fe + $Fe_{17}RE_2$ + liquid and $Fe_{17}RE_2$ + Fe_2RE + liquid, exist in the investigated region of the MM–Fe system. The γ-Fe phase cannot be retained by quenching the alloys from high temperature. The solid solubility of RE in iron is less than 0.5 at.%.

1. Introduction

During an investigation of the Fe–MM–B (MM, misch metal) system [1] it was observed that no 17:2 phase exists at 1000 °C in the ternary system, while three phases were found in Fe–MM alloys near the 17:2 stoichiometry. The presence of the α-Fe phase at 1000 °C is also somewhat unusual, since it is not found to be stable in any of the Fe–R binaries where R ≡ Ce, Nd, Pr or Sm [2]. All these observations have led us to a detailed study of the Fe–MM system at the iron-rich end.

2. Experimental procedure

Indian misch metal (from Raw Flints Pvt. Ltd., Rajkot) comprising 12% Fe, 1% impurities and 87% total rare earth (RE) content (the weight ratio of individual rare earth elements being Ce:La:Nd:Pr = 49:23:22:6) and 99.9% pure iron (supplied by Semi Elements Inc., New York) were arc melted under a high purity argon atmosphere. Thirteen alloys containing 0.5–33.3 at.% RE were prepared (Table 1). Since the melting loss in each case was less than 0.5%, the alloys were not chemically analysed. The alloy buttons were annealed in evacuated and sealed fused silica capsules in the temperature range between 700 and 1100 °C for time periods varying between 2 and 30 days (see Table 1) and finally quenched in water. Phase analysis of the annealed alloys was carried out using X-ray diffraction and metallographic techniques. An Iso-Debyeflex 2002 X-ray diffractometer fitted with a chromium target X-ray tube and a curved graphite crystal monochromator in the diffracted beam path was used at a slow scanning speed of 1.2° in 2θ per minute to obtain high resolution, β-reflection-free and practically background-free X-ray diffraction patterns. HNO_3 solution (1%–3%) was used as an etching reagent. A Stanton Redcroft DSC 1500 was used to determine the phase transformation temperatures of several alloys. A high temperature magnetic permeability tester [3] and a PAR 150A vibrating sample magnetometer fitted with a high temperature oven assembly were also used for phase identification and magnetic transition temperature determination.

3. Results and discussion

The results of the phase analysis done using X-ray diffraction and metallography are given in Table 1. No single-phase alloy was obtained in the present investigation. The presence of two intermediate phases, $Fe_{17}RE_2$ and Fe_2RE, was detected. Figure 1 shows the diffraction patterns of a series of alloys annealed at 900 °C. The characteristic features of the diffraction patterns of the phases present and their relative development in alloys with increasing RE content are shown in the diffraction patterns of alloys D_{00} (1 at.% RE) to D_2 (16.7 at.% RE) (Fig. 1). The lattice parameters of the $Fe_{17}RE_2$ and Fe_2RE phases were found to be $a = 0.8525$ nm, $c = 1.2420$ nm and $a = 0.7299$ nm respectively. When annealed at 900 °C, all alloys up to 13.5 at.% RE showed the presence of two phases, $Fe_{17}RE_2$ and α-Fe. The α-Fe phase was found to have a lattice parameter $a = 0.2869$ nm, which is very close to the lattice parameter of pure α-Fe. Thermomagnetic analysis of the alloy D_1 also confirmed the presence

0925-8388/92/$5.00

TABLE 1. Phase analysis of Fe–RE alloys

Alloy	Composition[a] (at.%)		Annealing		Phase Analysis	
	Fe	RE	Temperature (°C)	Time (days)	Metallography	X-ray
D_{000}	99.5	0.5	900	14	2 phase	α, 17:2
			1000	10	2 phase	α, 17:2
			1100	2	2 phase[b]	α
D_{00}	99.0	1.0	1000	10	2 phase	α, 17:2
			1100		2 phase[b]	α
			1150	1	2 phase[b]	α
D_0	98.0	2.0	900	14	2 phase	α, 17:2
			1000	4	3 phase[b]	α, 17:2
			1100	2	2 phase[b]	α
D_{12}	95.0	5.0	900	7	2 phase	α, 17:2
D_{13}	90.5	9.5	900	7	2 phase	α, 17:2
D_1	89.5	10.5	700	30	2 phase	α, 17:2
			800	8	2 phase	–
			900	16	2 phase	α, 17:2
			930	7	–	α, 17:2
			1000	3	3 phase[b]	α, 17:2
			1100	2	2 phase[b]	α
D_{1A}	88.5	11.5	800	7	2 phase	α, 17:2
			900	7	2 phase	α, 17:2
			1000	3	3 phase[b]	α, 17:2
D_{1B}	87.5	12.5	800	7	2 phase	α, 17:2
			900	7	2 phase	α, 17:2
			1000	6	3 phase[b]	α, 17:2
D_{1C}	86.5	13.5	800	7	2 phase	α, 17:2
			900	7	2 phase	α, 17:2
			1000	3	3 phase[b]	α, 17:2
D_2	83.3	16.7	700	30	2 phase	17:2. 2:1
			900	16	2 phase[b]	17:2
			1000	3	2 phase[b]	17:2
D_3	79.2	20.8	700	30	2 phase	17:2, 2:1
			900	6	2 phase[b]	17:2
			1000	3	2 phase[b]	17:2
D_4	77.8	22.2	700	30	2 phase	17:2. 2:1
			900	16	2 phase[b]	17:2
			1000	3	2 phase[b]	17:2
D_5	66.7	33.3	700	5	3 phase[b]	17:2, 2:1
			900	7	2 phase[b]	–
			1000	3	2 phase[b]	17:2

[a]Intended composition.
[b]One of the phases is a liquid phase.

of these two phases (Fig. 2(a)). As can be seen from the diffraction pattern (Fig. 1), the amount of α-Fe phase is quite small in the alloy D_{1C}. The alloy D_2 does not show the presence of the α-Fe phase (Fig. 1), but shows at 900 °C the presence of the $Fe_{17}RE_2$ phase (Fig. 1) and a liquid phase (Fig. 3). The weak additional diffraction lines in Fig. 1 can be identified as being due to the Fe_2RE phase arising out of the solidification of the liquid phase present in the alloy D_2 at 900 °C. Thus the $Fe_{17}RE_2$ phase region exists very close to the alloy D_{1C}, at a slightly higher RE content than the stoichiometric one. The chemical compositions of the alloys D_{1C} and D_2 and their microstructures suggest the $Fe_{17}RE_2$ phase region to be very narrow. That the $Fe_{17}RE_2$ phase region may have a small solubility limit at the lower temperatures is also indicated by the small difference in T_c of the alloy D_1 annealed at 900 and 700 °C (Fig. 2(b)). The alloys D_0 to D_{1C} at 1000 °C show the presence of three phases, α-Fe, $Fe_{17}RE_2$ and liquid, whereas the alloys D_{000} and

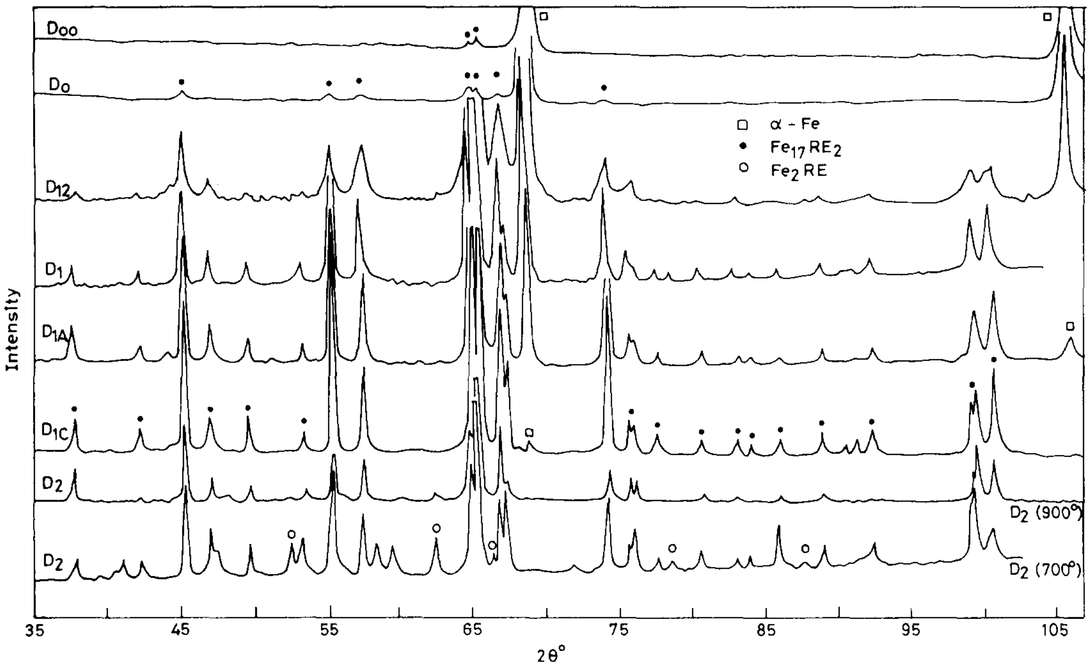

Fig. 1. X-ray diffraction patterns of a set of Fe–MM alloys annealed at 900 °C.

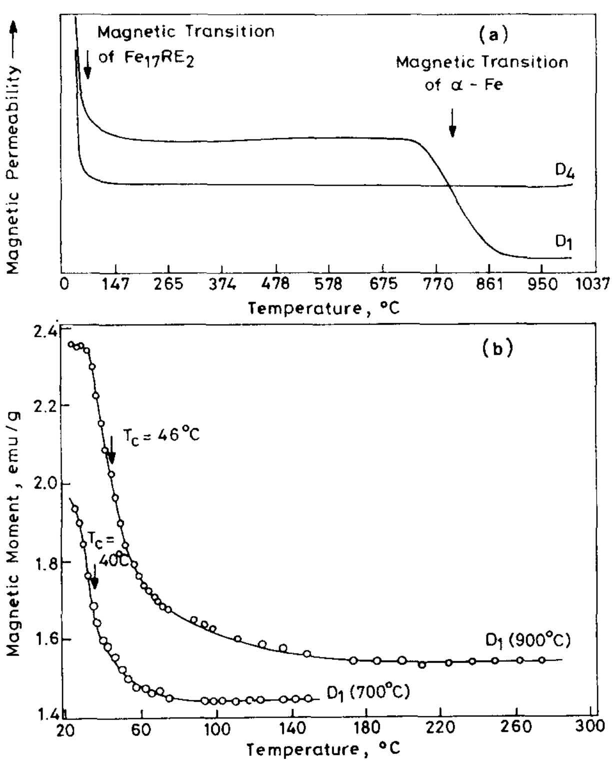

Fig. 2. Thermomagnetic analysis of alloys D_1 and D_4: (a) using a high temperature permeability tester; (b) using a vibrating sample magnetometer.

D_{00} showed the presence of only two phases, α-Fe and $Fe_{17}RE_2$. Annealing the alloys D_{000}, D_{00}, D_0 and D_1 at 1100 °C showed the presence of two phases, α-Fe and liquid. This indicates that between iron and the Fe–13.5 at.%RE alloy composition a reasonably wide

Fig. 3. Microstructure of alloy D_2 annealed at 900 °C and quenched in water (magnification, ×50).

three-phase field exists in the temperature range between 900 and 1100 °C. The alloy containing 0.5 at.% RE (alloy D_{000}) always showed two phases, one of which was the α-Fe phase irrespective of the annealing temperature used. Microstructural evidence and X-ray diffraction analysis thus indicate that the solubility of RE in iron is very small, less than 0.5 at.%. In order to see whether the α-Fe phase exists at all temperatures, differential scanning calorimetry (DSC) traces were obtained at a heating rate of 10 °C min^{-1} (Fig. 4). The DSC traces of alloys D_{000} to D_1 show the existence of a small thermal effect at about 770 °C, which is due

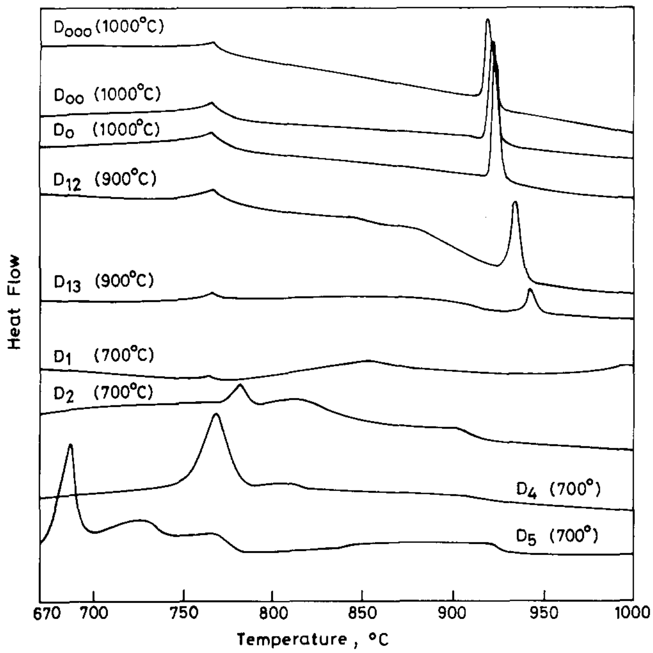

Fig. 4. DSC traces of a few Fe–MM alloys.

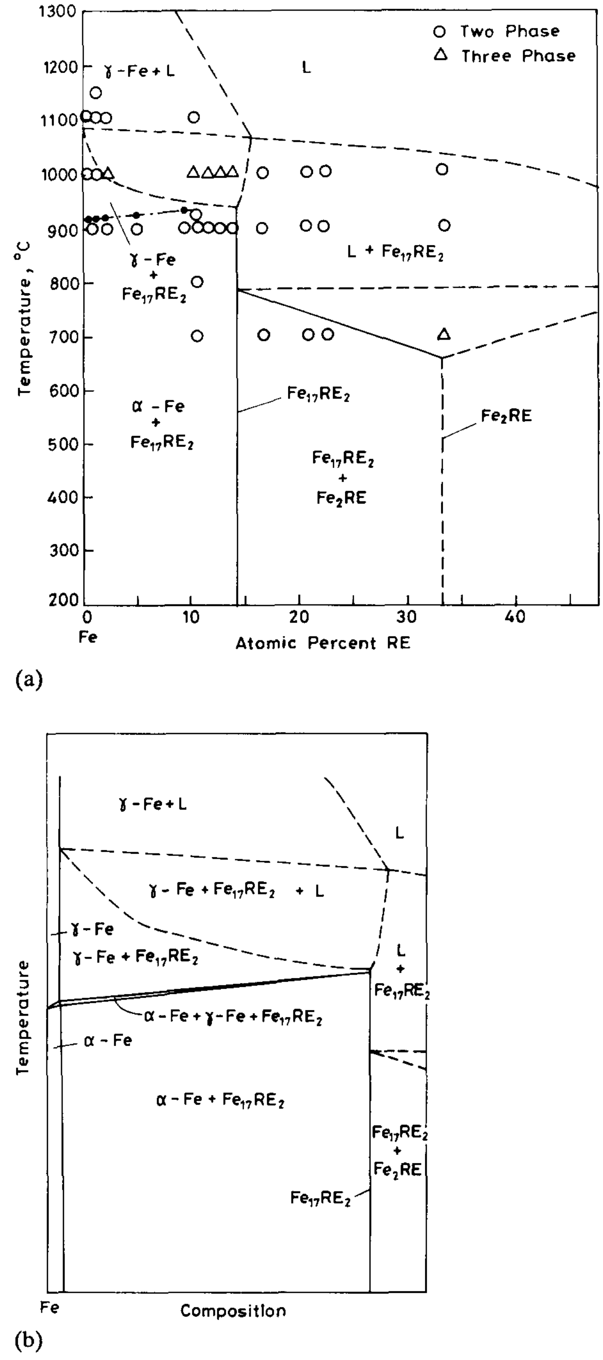

Fig. 5. (a) Phase equilibria in the Fe–MM system. (b) Schematic phase equilibria of the Fe–MM system showing a possible peritectoid-type reaction at the iron-rich end.

to the magnetic transition of the α-Fe phase, and a very sharp DSC peak occurs at a temperature higher than 912 °C. With increasing RE content of the alloys the latter DSC peak shifts to higher temperatures. For the alloy D_{13} this peak becomes very small and for the alloy D_1 it is non-existent. X-ray and metallographic observations indicate a decrease in α-Fe phase in the alloys from D_{13} to D_{1C}. The sharp DSC peak at $T > 912$ °C appears to be due to the α-Fe $\rightarrow$ γ-Fe transformation. The presence of the α-Fe phase in low RE alloys annealed above 950 °C appears to be due to the insuppressibility of the γ-Fe $\rightarrow$ α-Fe transformation by quenching in water.

When annealed at 900 °C, the alloys D_2, D_3, D_4 and D_5 showed the presence of two phases, $Fe_{17}RE_2$ and liquid, whereas on annealing at 700 °C, the first three alloys showed only two phases, $Fe_{17}RE_2$ and Fe_2RE, but the alloy D_5 contained three phases, $Fe_{17}RE_2$, Fe_2RE and liquid. The DSC trace of the alloy D_5 shows a sharp peak at about 670 °C and this temperature corresponds to the onset of melting of the alloy. With decreasing RE content of the alloys (D_4 to D_2) this thermal effect becomes small, owing to a lesser amount of liquid being formed, and appears at higher temperature. These temperatures may be used to determine approximately one side of the three-phase region containing the $Fe_{17}RE_2$, Fe_2RE and liquid phases.

When MM is alloyed with iron, the phases stabilized in the Fe–MM system are expected to be influenced by the elements present in the MM. The MM used is cerium based, the other rare earth elements present in it being lanthanum, neodymium and praseodymium. Of these rare earth elements, lanthanum does not give rise to any intermediate phase when alloyed with iron [2]. In the Fe–Ce and Fe–Pr systems two intermediate phases have been reported, $Fe_{17}R_2$ and Fe_2R [2, 4]. The Fe-Nd system on the other hand shows the presence of two intermediate phases, the $Fe_{17}Nd_2$ phase and the $Fe_{17}Nd_5$ phase which is stable below 777 °C [5, 6]. In the present investigation several alloys were annealed at 700 °C for 30 days. Even after this long annealing the alloys with greater than 15 at.% RE showed the presence of only two intermediate phases, $Fe_{17}RE_2$ and Fe_2RE; the $Fe_{17}RE_5$ phase was not observed. This indicates that in the presence of a very large amount of cerium (and also owing to praseodymium) the 2:1 phase is stabilized in preference to the 17:5 phase.

On the basis of the phase analysis data, the phase equilibria at the iron end of the Fe–RE system may be arrived at and are given in Fig. 5(a). For the high iron alloys the DSC data suggest the occurrence of the $\alpha \rightarrow \gamma$ transformation at temperatures slightly higher than 912 °C (shown by the chain line in Fig. 5(a)). In the R–Fe systems an invariant reaction occurs at 912 °C or at a slightly higher temperature. In the Nd–Fe system this invariant reaction has been identified as a peritectoid reaction, γ-Fe + $Fe_{17}Nd_2 \rightleftharpoons \alpha$-Fe, the reaction temperature being 935 °C [2]. DSC study of the alloy D_{000} (0.5 at.% RE) shows the α-Fe $\rightarrow \gamma$-Fe transformation at about 915 °C and for alloys with higher RE content this reaction temperature increases. It may be possible to interpret the phase equilibria in the low RE content region of the Fe–RE system if it is assumed that the α-Fe forms through a similar peritectoid-type reaction to the Nd–Fe system, giving rise to a very narrow three-phase region, α-Fe + γ-Fe + $Fe_{17}RE_2$, as shown schematically in Fig. 5(b).

4. Conclusions

Phase equilibria studied at the iron-rich end of the MM–Fe system show the presence of two intermediate phases, $Fe_{17}RE_2$ and Fe_2RE, where RE stands for the total rare earth content of the MM, which are stable below about 950 and 670 °C respectively. The α-Fe phase in all quenched (from $T > 950$ °C) iron-rich alloys is due to the transformation of γ-Fe to α-Fe, and possibly a narrow three-phase region, α-Fe + γ-Fe + $Fe_{17}RE_2$, exists. Two reasonably wide three-phase fields, γ-Fe + $Fe_{17}RE_2$ + liquid and $Fe_{17}RE_2$ + Fe_2RE + liquid, exist in the MM–Fe system.

References

1 M. Uma Devi and K. P. Gupta, *J. Less-Common Met., 159* (1990) 13.
2 T. B. Massalski, *Binary Alloy Phase Diagrams,* American Society for Metals, Metals Park, OH, 1986.
3 V. Manuja, M. Uma Devi and K. P. Gupta, in S. P. Mehrotra and T. R. Ramachandran (eds.), *Progress in Metallurgical Research: Fundamental and Applied Aspects,* Tata McGraw-Hill, New Delhi, 1986, p. 415.
4 Y. C. Chuang, C. H. Wu and Z. B. Shao, *J. Less-Common Met., 136* (1987) 147.
5 G. Schneider, F. J. G. Landgraf and F. P. Missell, *J. Less-Common Met., 153* (1989) 169.
6 F. J. G. Landgraf, G. S. Schneider, V. Villas-Boas and F. J. Missell, *J. Less-Common Met., 163* (1990) 209.